Neurotherapeutics (2015) 12:234–249
DOI 10.1007/s13311-014-0305-y

ORIGINAL ARTICLE

# The Riluzole Derivative 2-Amino-6-trifluoromethylthio-benzothiazole (SKA-19), a Mixed $K_{Ca}2$ Activator and $Na_V$ Blocker, is a Potent Novel Anticonvulsant

**Nichole Coleman · Hai M. Nguyen · Zhengyu Cao · Brandon M. Brown · David Paul Jenkins · Dorota Zolkowska · Yi-Je Chen · Brian S. Tanaka · Alan L. Goldin · Michael A. Rogawski · Isaac N. Pessah · Heike Wulff**

Published online: 26 September 2014


**Abstract** Inhibitors of voltage-gated sodium channels ($Na_v$) have been used as anticonvulsants since the 1940s, while potassium channel activators have only been investigated more recently. We here describe the discovery of 2-amino-6-trifluoromethylthio-benzothiazole (SKA-19), a thioanalog of riluzole, as a potent, novel anticonvulsant, which combines the two mechanisms. SKA-19 is a use-dependent $Na_V$ channel blocker and an activator of small-conductance $Ca^{2+}$-activated $K^+$ channels. SKA-19 reduces action potential firing and increases medium afterhyperpolarization in CA1 pyramidal neurons in hippocampal slices. SKA-19 is orally bioavailable and shows activity in a broad range of rodent seizure models. SKA-19 protects against maximal electroshock-induced seizures in both rats ($ED_{50}$ 1.6 mg/kg i.p.; 2.3 mg/kg p.o.) and mice ($ED_{50}$ 4.3 mg/kg p.o.), and is also effective in the 6-Hz model in mice ($ED_{50}$ 12.2 mg/kg), Frings audiogenic seizure-susceptible mice ($ED_{50}$ 2.2 mg/kg), and the hippocampal kindled rat model of complex partial seizures ($ED_{50}$ 5.5 mg/kg). Toxicity tests for abnormal neurological status revealed a therapeutic index ($TD_{50}/ED_{50}$) of 6–9 following intraperitoneal and of 33 following oral administration. SKA-19 further reduced acute pain in the formalin pain model and raised allodynic threshold in a sciatic nerve ligation model. The anticonvulsant profile of SKA-19 is comparable to riluzole, which similarly affects $Na_V$ and KCa2 channels, except that SKA-19 has a ~4-fold greater duration of action owing to more prolonged brain levels. Based on these findings we propose that compounds combining KCa2 channel-activating and $Na_v$ channel-blocking activity exert broad-spectrum anticonvulsant and analgesic effects.

**Keywords** Anticonvulsant · Voltage-gated sodium channel · Calcium-activated potassium channel · Afterhyperpolarization · Seizure models · Riluzole

N.C. and H.M.N. contributed equally to this work.

N. Coleman · H. M. Nguyen · B. M. Brown · D. P. Jenkins · Y.-J. Chen · H. Wulff (✉)
Department of Pharmacology, Genome and Biomedical Sciences Facility, School of Medicine, University of California, 451 Health Sciences Drive, Davis, CA 95616, USA
e-mail: hwulff@ucdavis.edu

Z. Cao
State Key Laboratory of Natural Medicines, China Pharmaceutical University, Nanjing, People's Republic of China

D. Zolkowska · M. A. Rogawski
Department of Neurology, School of Medicine, University of California, Davis, CA, USA

B. S. Tanaka · A. L. Goldin
Department of Microbiology and Molecular Genetics, School of Medicine, University of California, Irvine, CA, USA

I. N. Pessah
Department of Molecular Biosciences, School of Veterinary Medicine, University of California, Davis, CA, USA

## Introduction

Epilepsy, a complex neurological disorder estimated to affect over 50 million people worldwide, is characterized by recurrent spontaneous seizures due to neuronal hyperexcitability and hypersynchronous neuronal firing. Despite the availability of more than 20 antiepileptic drugs (AEDs) about 30 % of patients with epilepsy continue to experience seizures or suffer from unacceptable drug side effects [1, 2]. Therefore, there remains a substantial unmet need to identify AEDs with novel mechanisms of action that could be used either in

monotherapy or integrated into combination regimens to obtain adequate seizure control for presently pharmacoresistant patients.

In general, there are currently three approaches for identifying new AEDs [1]. The first approach, which is intellectually most satisfying, is mechanism based: drugs are specifically developed to modify the function of molecular targets believed to be relevant to human epilepsy based on human mutations and/or genetic manipulations in rodents. An example is the ongoing search for potent and selective Kv7.2/7.3 (KCNQ2/3) activators like ICA-27243, ICA-105665 or other retibagine-related compounds [3–5]. These chemistry programs were initated based on the observation that loss-of function mutations in Kv7.2 (KCNQ2) have been associated with benign familial neonatal convulsions, a rare hereditary form of human epilepsy [6]. The second approach is to design follow-on compounds to existing AEDs with more favorable side effects or pharmacokinetic profiles, such as eslicarbazepine acetate as a third-generation follow-on drug to carbamazepine. The third approach, which has been pursued by the National Institutes of Health's (NIH) Anticonvulsant Screening Program (ASP) since 1975, is empirical and uses rodent screening models. We here used a serendipitous combination of all 3 approaches to identify 2-amino-6-trifluoromethylthio-benzothiazole (SKA-19), a thioanalog of riluzole, as a potent, novel anticonvulsant (Fig. 1).

Riluzole, a compound first mentioned as a new chemical entity in a Russian-language publication on diazastyrenes dyes in 1963, was reported by scientists at Rhone Poulenc in 1985 to exhibit anticonvulsant effects in rodents and baboons [7]. Overall, the anticonvulsant spectrum seemed to be phenytoin-like and similar to other sodium channel-blocking AEDs [8]. Riluzole was subsequently extensively studied as a neuroprotective agent. In 1995, the US Food and Drugs Administration approved the use of riluzole, which is marketed under the trade name Rilutek (Sanofi-Aventis, Bridgewater, NJ, USA), for the treatment of amyotrophic lateral sclerosis and it still remains the only drug able to prolong survival in this fatal neurodegenerative condition [9]. Interestingly, despite being widely studied, riluzole had never been evaluated in the NIH ASP until our laboratory recently submitted it. Riluzole exhibits various pharmacological activities, the most prominent of which are inhibition of voltage-gated $Na^+$ ($Na_V$) channels at concentrations of 1–50 μM and activation of small-conductance $Ca^{2+}$-activated $K^+$ channels with $EC_{50}$s of 10–20 μM [10, 11]. Riluzole has further been reported to inhibit delayed-rectifier $K^+$ channels and to activate 2-pore $K^+$ channels at 30–100 μM [12]. Riluzole's relatively high potency as an activator of calcium-activated $K^+$ channels (KCa) and its good pharmacokinetic properties rendered it an attractive template for the design of KCa channel modulators. Accordingly, our laboratory performed a structure–activity study of the riluzole pharmacophore and developed a series of compounds exemplified by SKA-31, which activates intermediate-conductance KCa3.1 and small-conductance KCa2 channels with $EC_{50}$ values of 250 nM or 2 μM, but was devoid of any significant $Na_V$ channel-blocking activity [13]. As KCa2 channels are expressed in the hippocampus, amygdala, and cerebellum [14], where they participate in the regulation of neuronal after-hyperpolarization and excitability, and also serve as negative feedback regulators on the glutamate–*N*-methyl-D-aspartate pathway, KCa2 channel activators have been proposed for the treatment of central nervous system (CNS) disorders that are characterized by hyperexcitability such as epilepsy and ataxia [15]. As such, we submitted SKA-31 and several of its derivatives to the NIH's ASP, where they were found to be effective in the maximal electroshock (MES) seizure model, the 6-Hz seizure model, and in the hippocampal kindled rat model. However, together with our relatively well characterized KCa2 channel activators we submitted several less well characterized riluzole derivatives and found SKA-19 to be a potent, orally active anticonvulsant. SKA-19 also reduced the acute pain response in the formalin pain model and raised the allodynic threshold in a sciatic nerve ligation model. Mechanism of action studies showed that SKA-19 suppresses $Ca^{2+}$ oscillations in cultured hippocampal neurons induced by picrotoxin (PTX) and 4-aminopyridine (4-AP); reduces firing frequency and increases medium after-hyperpolarization currents in hippocampal slices; and inhibits $Na_v$ channels, as well as activates KCa2 channels at low micromolar concentrations. Based on these findings we propose that compounds combining KCa2 channel-activating and state-dependent $Na_v$ channel blocking activity exert broad-spectrum anticonvulsant and analgesic effects.

## Materials and Methods

### Drugs

SKA-19 (CAS 326-45-4) and riluzole (CAS 1744-22-5) were purchased from Oakwood Products (West Columbia, SC,

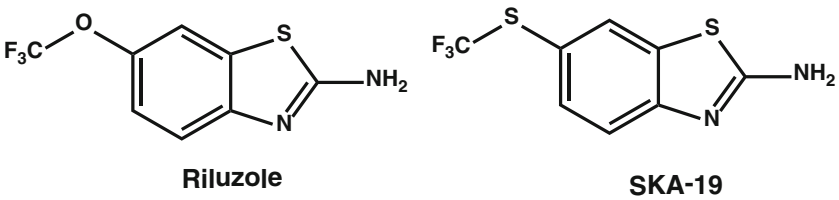


**Fig. 1** Chemical structures of riluzole and 2-amino-6-trifluoromethylthio-benzothiazole (SKA-19)

USA) and recrystallized in our laboratory. $^{1}H$ and $^{13}C$ nuclear magnetic resonance were used to confirm identity and purity.

## Seizure Tests

SKA-19 and riluzole were tested under the auspices of the NIH's ASP. Experiments were performed in male albino Carworth Farms No. 1 (CF-1) mice or Sprague–Dawley rats according to the established protocols of the ASP [16]. SKA-19 and riluzole were suspended in 0.5 % methylcellulose and administered in a volume of 0.01 ml/g body weight for mice and 0.04 ml/10 g body weight for rats.

## MES Test

Animals received an electrical stimulus for 0.2 s (50 mA for mice and 150 mA for rats) at 60 Hz delivered via corneal electrodes. In the initial screens, mice were tested at 30 min and 4 h, and rats at time intervals between 0.25 and 4 h after test compound application. In the subsequent, quantitative tests at least 4 doses of SKA-19 ($n$=8 animals per dose) were tested at the previously determined time of peak effect (TPE). Abolition of hindlimb tonic extension indicates the test compound's ability to inhibit MES-induced seizure spread.

The MES testing (see Fig. 5) was performed at the Department of Neurology, University of California, Davis, and utilized male NIH Swiss mice (22–30 g) were obtained from the Animal Resource Program, National Cancer Institute (Bethesda, MD, USA). SKA-19 was solubilized in 5 % CremophorEL (Sigma-Aldrich, St. Louis, MO, USA) and 95 % saline to provide a clear, 5-mg/ml stock solution. Riluzole (5 mg/ml) was prepared in 10 % Captisol (Ligand Technology, La Jolla, CA, USA) and 90 % saline. Both stocks were diluted further with saline, and SKA-19 and riluzole were administered intraperitoneally (i.p.) as a clear solution in a volume of 10 ml/kg body weight. Animals were subjected to a 0.2-s, 60-Hz electrical stimulus through corneal electrodes (50 mA). Animals failing to show tonic hindlimb extension were scored as protected [17].

## Subcutaneous Pentylenetetrazol (PTZ) Seizure Test

A dose of subcutaneous pentylenetetrazol (PTZ), which induces convulsions in 97 % of animals (CD97: 85 mg/kg mice or 56.4 mg/kg rats), was injected into a loose fold of skin at the neck. Animals were placed in isolation cages and observed for 30 min for the occurrence of clonic spasms persisting for at least 5 s. Test compound was administered i.p. or through oral dosing at various times before PTZ. Animals not exhibiting seizures were considered protected.

## 6-Hz Seizure Test

Seizures characterized by a minimal clonic phase followed by stereotyped automatistic behaviors were induced in mice by a low frequency (6 Hz), long-duration (3 s) stimulus delivered through corneal electrodes. At varying times (0.25, 0.5, 1, 2, and 4 h) after drug treatment, individual mice (4 at each time point) were challenged with a current of either 32 or 44 mA. Animals not displaying this behavior were considered protected.

## Hippocampal Kindled Seizures

Bipolar electrodes were surgically implanted into the hippocampus of anesthetized male rats. One week after the surgery, rats were stimulated with suprathreshold trains of 200 μA for 10 s, 50 Hz, every 30 min for 6 h (12 stimulations per day) on alternate days until they were fully kindled. One week later the effect of a single i.p. dose of test compound was assessed on behavioral seizure score and afterdischarge duration. An initial group of kindled rats ($n$=6–8) were tested at 15, 45, 75, 105, 135, 165, and 195 min after drug administration. Results were compared with the last control stimulus delivered 15 min prior to drug administration. Thus, each animal served as its own control. Scoring was performed as follows: stage 1= mouth and facial clonus; stage 2=stage 1 plus head nodding; stage 3=stage 2 plus forelimb clonus; stage 4=stage 3 plus rearing; stage 5=stage 4 plus repeated rearing and falling.

## Frings Audiogenic Seizure-susceptible Mice

Frings audiogenic seizure (AGS)-susceptible mice are genetically susceptible to sound-induced seizures [18]. A colony of AGS mice is maintained by the ASP at the University of Utah. Groups of 8 female mice (weighing 18–25 g) were treated i.p. with increasing doses of SKA-19. At the TPE in the MES test, mice were exposed to a sound stimulus of 110 decibels (11 KHz) delivered for 20 s. Mice were observed for the presence or absence of hindlimb tonic extension.

## Intravenous PTZ Infusion Test

The intravenous (i.v.) PTZ test provides a measure of a test substance's ability to raise or lower seizure threshold. Two doses of the test compound are employed in this test, the MES $ED_{50}$ and the $TD_{50}$, determined following i.p. quantification testing in mice. Accordingly, SKA-19 was tested at 5 and 30 mg/kg. Randomly selected male mice ($n$=30) were injected i.p. 2 min apart with either the vehicle or the 2 test drug doses. At the previously determined TPE, 0.5 % heparinized PTZ solution was infused at a constant rate into a lateral tail vein. The time in seconds from the start of the infusion to the appearance of the "first twitch" and the onset

of sustained clonus is recorded. The times to each endpoint are converted to mg/kg of pentylenetetrazol for each mouse. The mean (SE) for each of the 3 groups and the significance of the difference between the test groups and the control were calculated.

### Test for Neurotoxicity

Abnormal neurological status in mice following the administration of SKA-19 and riluzole was evaluated with the rotorod test and the horizontal screen test as previously described [16]. For the experiment shown in Fig. 5, motor impairment was evaluated using a modification of the horizontal screen test as previously described [17]. Abnormal neurological status in rats was evaluated by the positional sense test, the muscle tone test, and the gait and stance test.

### Statistical Analysis

$ED_{50}$s and $TD_{50}$ values were calculated by a FORTRAN probit analysis program, which provides the 95 % confidence intervals (CIs), the slope of the regression lines, and the SE of the slopes. For the experiments shown in Fig. 5 a similar log–probit analysis was performed to calculate $ED_{50}$, $TD_{50}$, and 95 % CIs with the Litchfield and Wilcoxon method (PHARM/PCS Version 4.2; Micro-Computer Specialists, Philadelphia, PA, USA).

### Pain Assays

#### *Formalin Pain Assay*

SKA-19 was administered at a dose of 5 mg/kg to CF-1 male mice. At the previously determined time of peak anticonvulsant effect, 0.5 % formalin was injected subdermally into the plantar surface of the right hindfoot. For each animal the amount of time (s) spent licking the affected hind paw in a 2-min period was recorded at 5-min intervals and continued for 45 min through both the acute and inflammatory phase.

#### *Partial Ligation of the Sciatic Nerve*

Male rats were anesthetized with sodium pentobarbital, the sciatic nerve exposed, and approximately one-third to one-half of the nerve tied off. This procedure was performed on the right side (ipsilateral), while a sham surgery exposing, but not ligating, the nerve was performed on the left hindleg (contralateral). After 7 days of recovery animals were tested for the development of mechanical allodynia by placing them on a wire mesh (1/4") platform. After 30–60 min of acclimatization a baseline mechanical sensitivity was determined by applying a series of calibrated Von Frey fibers perpendicularly to the plantar surface of each hindpaw. After a positive response (withdrawal of the foot) was noted a weaker fiber was applied. This was repeated until a 50 % threshold for withdrawal could be determined. The allodynic threshold was then redetermined after i.p. application of SKA-19 at 5 mg/kg.

### Pharmacokinetics

All experiments were approved by the University of California, Davis, Institutional Animal Care and Use Committee. Nine–11-week-old male Sprague–Dawley rats were purchased from Charles River Laboratories (Wilmington, MA, USA). For i.v. application, SKA-19 was dissolved at 5 mg/ml in a mixture of 10 % CremophorEL (Sigma-Aldrich) and 90 % phosphate-buffered saline (Sigma-Aldrich, St. Louis, MO, USA), and then injected at 10 mg/kg into the tail vein. At various time points after the injection, ~100–200 μl blood was collected from a tail nick. Plasma was separated by centrifugation and stored at –80 °C. For i.p. application, SKA-19 was dissolved in Miglyol 812 neutral oil (caprylic/capric triglyceride; Neobee M5, Spectrum Chemicals, Gardena, CA, USA) at 2 mg/ml and injected at 10 and 30 mg/kg. After determining that SKA-19 plasma concentrations peaked 2 h after i.p. application, 2 groups of rats ($n$=3 per group) received 10 mg/kg SKA-19 or riluzole, were subjected to cardiac puncture under deep isoflurane anesthesia 2 h later and then sacrificed before removing brain, heart, liver, spleen, and fat. Tissue samples were homogenized in 1 ml $H_2O$ with a Brinkman Kinematica PT 1600E (KINEMATICA, INC., Bohemia, NY) homogenizer and the protein precipitated with 1 ml of acetonitrile. The samples were then centrifuged at 1620 g and supernatants concentrated to 1 ml. Plasma and homogenized tissue samples were purified using $C_{18}$ solid phase extraction cartridges. Eluted fractions corresponding to SKA-19 were dried under nitrogen and reconstituted in acetonitrile. Liquid chromatography/mass spectrometry (MS) analysis was performed with a Waters Acquity UPLC (Waters, Parsippany, NJ, USA) equipped with a Acquity UPLC BEH 1.7-μm RP-18 column interfaced to a TSQ Quantum Access Max MS (ThermoFisher Scientific, Waltham, MA, USA). The mobile phase consisted of acetonitrile and water, both containing 0.1 % formic acid. With a flow rate of 0.25 ml/min, the gradient was ramped from 95 % water to 95 % acetonitrile. Using electrospray ionization MS and selective reaction monitoring (capillary temperature 350 °C, capillary voltage 4000 V, collision energy –26 eV, positive ion mode), SKA-19 was quantified by its base peak of 182.9 m/z ($C_7H_7N_2S_2^+$ fragment) and its concentration was calculated with a 9-point calibration curve from 50 nmol/l to 10 μmol/l. The percentage of plasma protein binding for SKA-19 was determined by ultrafiltration and was found to be 81.2±1.1 % ($n$=3). Very similar results [83±1.1 % ($n$=2)] were obtained by equilibrium dialysis.

### Primary Cultures of Hippocampal Neurons

Brains were harvested from C57Bl/6 J mouse pups at postnatal day 0–1 in accordance with NIH guidelines and following approval by the University of California, Davis, Institutional Animal Care and Use Committee. Hippocampal neurons were dissociated from dissected hippocampi, plated onto a poly-L-lysine-coated clear-bottom, black wall, 96-well imaging plate (BD, Franklin Lakes, NJ, USA) at a density of $0.8 \times 10^5$ cells/well, and maintained in Neurobasal (Life Technologies, Grand Island, NY) complete medium (Neurobasal medium supplemented with NS21, 0.5 mM L-glutamine, HEPES; Sigma-Aldrich) with 5 % fetal bovine serum (Life Technologies, Gibco$^R$). On day 2 *in vitro*, cytosine arabinoside (10 μM) was added to the culture to suppress the growth of astrocytes. Starting at 5 days *in vitro* (DIV), the medium was changed twice a week by replacing half the volume of culture medium in the well with serum-free Neurobasal complete medium.

### Measurement of Synchronous Intracellular $Ca^{2+}$ Oscillations

Hippocampal neurons 14–17 DIV were used for simultaneous measurements of intracellular $Ca^{2+}$ transients in all wells of a 96-well plate as described previously [19]. After aspiration, the cells were incubated with 4 μM Fluo-4 in Locke's buffer containing 0.5 mg/ml bovine serum albumin for 1 h at 37 °C. The plates were then transferred to the FLIPR (Molecular Devices, Sunnyvale, CA, USA) cell plate stage. After 4 min of baseline recordings, $Ca^{2+}$ signals were then recorded for 10 min in the presence or absence of SKA-19 followed by addition of the $Ca^{2+}$ enhancing agents 4-AP or PTX, and the intracellular $Ca^{2+}$ concentration ($[Ca^{2+}]_i$) was monitored for an additional 30 min. $Ca^{2+}$-enhancing agents triggered an immediate rise in $[Ca^{2+}]_i$ that was quantified by determining the area under the curve of the Fluo-4 arbitrary fluorescence units for a duration of 5 min following agent addition.

### Slice Recordings

Brain slice preparation was approved by the University of California, Irvine, Institutional Animal Care and Use Committee. Male C57BL/6 J mice (postnatal day 23) were anesthetized with halothane, decapitated, and brains transferred to an ice-cold, sucrose artificial cerebral spinal fluid (ACSF; Sigma-Aldrich). Hippocampal slices (300 μm) were prepared using a Leica VT1200S vibrating blade microtome (Leica Microsystems Inc., Buffalo Grove, IL). Slices were incubated at 33 °C in oxygenated (95 % $O_2$, 5 % $CO_2$) standard ACSF containing the following (mM) for at least 1 h before recordings: 126 NaCl, 2.5 KCl, 1.25 $NaHPO_4$, 1.2 $MgSO_4$, 10 glucose, 1.2 $CaCl_2$, and 26 $NaHCO_3$ . Slices were submerged and continuously perfused at 2 ml/min with oxygenated ACSF at 33 °C during the current–clamp experiments. Voltage–clamp experiments were performed in the same ACSF but with 1 mM tetraethylammonium chloride (Sigma-Aldrich) and 0.5 μM tetrodotoxin (Sigma-Aldrich) added. Pyramidal CA1 neurons were visualized and identified with an upright microscope (Zeiss Axioskop Plus; Zeiss Jena, Germany) with infrared differential interference contrast optics. Recording pipettes (2–5 MΩ) were filled with intracellular solution containing (in mM): 126 K-gluconate; 4 KCl; 10 HEPES; 2 Mg–adenosine triphosphate; 0.3 Tris–guanosine triphosphate; 10 phosphocreatine, pH 7.20, 270–290 mOsm. In the current–clamp mode, depolarizing current pulses were applied from a membrane potential of −65 mV to evoke tonic firing activity. In the voltage–clamp mode, neurons were held at –55 mV and KCa currents elicited by 50-ms voltage steps to 10 mV, applied every 10 s. SKA-19 or NS309 were perfused for 10 min into the bath to allow for equilibrium. Recordings were performed in the whole-cell mode using a MultiClamp 700B amplifier (Molecular Devices), digitized at 4 kHz and sampled at 20 kHz with a Digidata 1322A digitizer (Molecular Devices). Data were acquired and analyzed with pClamp 10.2 software (Molecular Devices).

### Voltage–Clamp Experiments

All experiments were conducted at room temperature (22–24 °C) with an EPC-10 amplifier and Pulse software (HEKA, Lambrecht/Pfalz, Germany) in the whole-cell mode of the patch–clamp technique. Human embryonic kidney (HEK)-293 cell lines stably expressing $hNa_V1.1$, $hNa_V1.5$, $hNa_V1.7$ channels (generously provided by Dr. Christopher Lossin, University of California Davis), $hNa_V1.4$ (Frank Lehmann-Horn, University of Ulm), or $hK_V2.1$ channels (James Trimmer, University of California Davis) were bathed in extracellular solution containing (in mM): 160 NaCl; 4.5 KCl; 1 $MgCl_2$; 2 $CaCl_2$; 10 HEPES [pH was adjusted to 7.4 using NaOH (310 mOsm)]. Pipettes were filled with intracellular solution containing (in mM): 145 KF; 2 $MgCl_2$; 10 ethylene glycol tetraacetic acid; 10 HEPES (pH adjusted to 7.2 with KOH; 300 mOsm). Neuroblastoma N1E-115 cells (ATCC, Manassa, VA, USA) expressing $Na_V1.2$ were patched with a CsF internal solution consisting of (in mM): 10 NaF; 110 CsF; 20 CsCl; 2 ethylene glycol tetraacetic acid; 10 HEPES (CsOH to pH 7.35; 300 mOsm). All pipette tip resistances were 2–4 MΩ. Series resistances of 3–10 MΩ were compensated 40–80 %. All cells were voltage-clamped to a holding potential of –90 mV unless otherwise specified. The sampling frequency was 5 kHz. $Na^+$ currents were elicited by 30-ms pulse to 0 mV from –90 mV applied every 10 s. $K_V2.1$ currents were elicited by 200-ms voltage steps from –90 to 40 mV applied every 10 s.

HEK-293 or COS-7 cells stably expressing hKCa2.1, rKCa2.2, and hKCa2.3 have been described previously [13]. Cells were held at –80 mV and KCa currents elicited by dialysis with a $K^+$ aspartate based internal containing

250 nM free $Ca^{2+}$ (pH 7.2, 290 mOsm, pipette resistance 1.5 MΩ). To reduce currents from native chloride channels, $Na^{+}$ aspartate Ringer was used as an external solution. KCa2 currents were recorded with 200-ms voltage ramps from –120 to +40 mV applied every 10 s, and the fold increase of slope conductance at –80 mV by drug was taken as a measure of channel activation. Data analysis, fitting, and plotting were performed with IGOR-Pro (Wavemetrics, Lake Oswego, OR, USA) and Origin 9.0 (OriginLab, Northampton, MA, USA).

## Results

### SKA-19 is Active in the MES Seizure Test

SKA-19 was evaluated for antiseizure activity in the initial qualitative screens of the ASP, which are used for routine identification of potential novel anticonvulsants. These so-called "identification" tests evaluate a compound at increasing doses in the MES and the subcutaneous PTZ tests combined with an initial assessment of toxicity in the rotorod test. SKA-19 fully protected mice in the MES model following i.p. administration at 10, 30, and 100 mg/kg, and exhibited partial protection at 3 mg/kg. However, it did not provide any protection in the PTZ test at 30 and 100 mg/kg, while one animal treated with 300 mg/kg died in the PTZ test without exhibiting a seizure. Preliminary toxicity testing for neurological deficits revealed no impairment of motor performance in the rotorod test at 0.5 and 4 h after doses of 3, 10, and 30 mg/kg, but showed inability to clasp the rotorod at 100 mg/kg, and sedation or death at 300 mg/kg. Following oral administration at 30 mg/kg, SKA-19 also fully protected rats in the MES test at all time points (0.25, 0.5, 1, 2, and 4 h) without inducing motor impairment ($n$=4).

As this initial screen showed activity in the MES test in 2 species and an encouraging difference between efficacy and neurotoxicity, we next evaluated SKA-19 quantitatively. When tested for seizure protection in the MES test following i.p. administration at 4 doses ($n$=8 per dose) SKA-19 was found to have an $ED_{50}$ of 4.8 mg/kg [95 % confidence interval (CI) 4.05–5.37] in mice and an $ED_{50}$ of 1.6 mg/kg (95 % CI 1.24–1.94) in rats (Fig. 2). Simultaneously performed testing for motor impairment revealed a $TD_{50}$ for affecting the ability of mice to stay on the rotorod of 29.8 mg/kg (95 % CI 25.35–35.98; 6 doses, $n$=8 per dose). At 100 mg/kg 2/8 mice died.

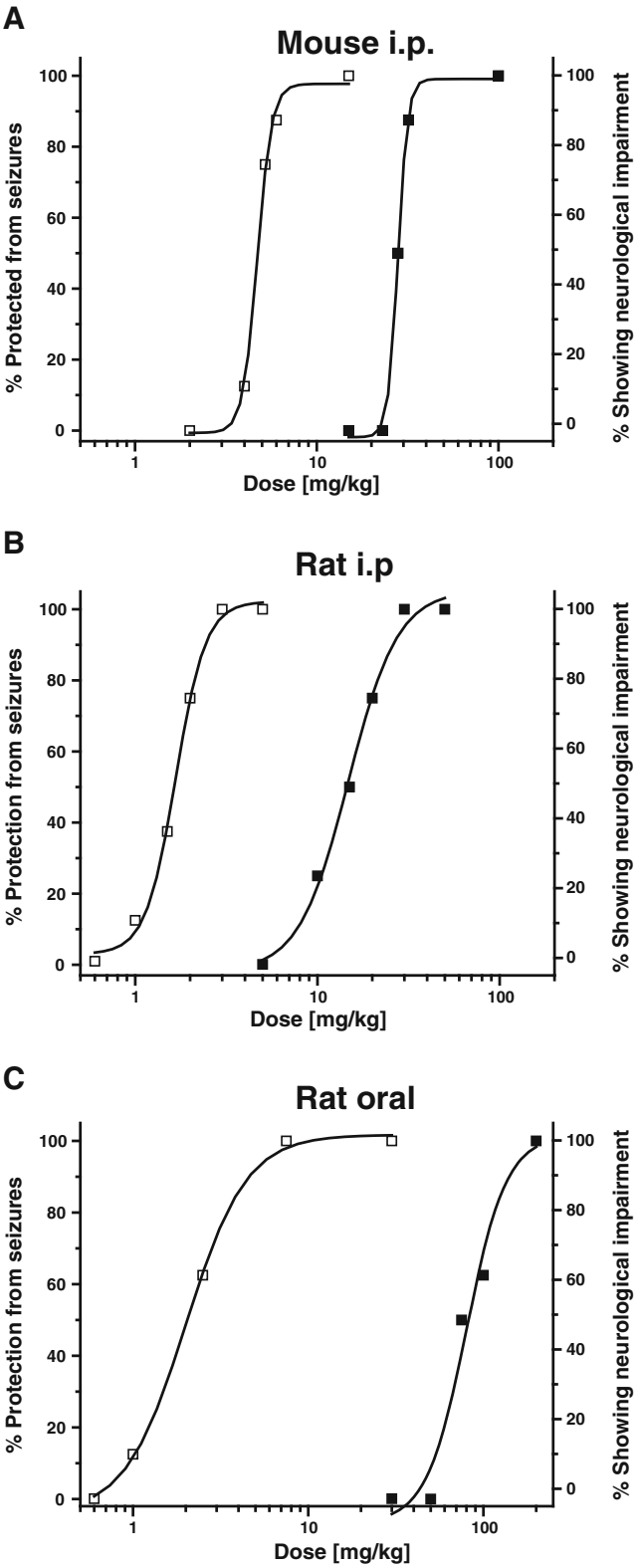


**Fig. 2** 2-Amino-6-trifluoromethylthio-benzothiazole (SKA-19) protects mice and rats in the maximal electroshock (MES)-induced seizure model. (**a**) Dose–response curves for seizure protection in the MES test (□) and neurological impairment (■) following intraperitoneal (i.p.) administration in mice ($n$=8 per dose, 2-h time point). $ED_{50}$ 4.8 mg/kg [95 % confidence interval (CI) 4.05–5.37], $TD_{50}$ 29.8 mg/kg (95 % CI 25.35–35.98); protective index (PI) 6.2. (**b**) Dose–response curves for i.p. administration in rats ($n$=8 per dose, 1-h time point). $ED_{50}$ 1.6 mg/kg (95 % CI 1.24–1.94), $TD_{50}$ of 14.33 mg/kg (95 % CI 10.72–17.9); PI 8.9. (**c**) Dose–response curves for oral administration in rats ($n$=8 per dose, 4-h time point). $ED_{50}$ 2.33 mg/kg (95 % CI 1.3–3.39), $TD_{50}$ 77.38 mg/kg (95 % CI 62.55–91.01); PI 33.2

The neurological status of rats was determined by their ability to perform normally in 3 simple neurological tests; SKA-19 impaired the neurological function with a $TD_{50}$ of 14.33 mg/kg (95 % CI 10.72–17.9; 5 doses, $n$=8 per dose). Taken together, these tests rendered a therapeutic ($TD_{50}/ED_{50}$) or protective index (PI) of 6.2 for mice and of 8.9 for rats following i.p. application. As is generally the case, the PI was found to be considerably higher (~33) following oral application in rats (Fig. 2) which rendered an $ED_{50}$ in the MES test of 2.33 mg/kg (95 % CI 1.30–3.39; 4 doses, $n$=8 per dose) and a $TD_{50}$ of 77.38 mg/kg (95 % CI 62.55–91.01). No deaths occurred in rats at higher doses. Similar findings were made following oral application in mice (data not shown; MES $ED_{50}$ 4.31 mg/kg, $TD_{50}$ 78.63 mg/kg).

Interestingly, when we subsequently submitted riluzole to the ASP, this clinically used drug was found to exhibit a surprisingly high toxicity when given i.p.. In the initial screen, riluzole already affected rotorod performance and righting reflexes in 8/8 mice at 30 mg/kg and killed 8/8 mice at 100 mg/kg following i.p. application. In rats, a dose of 30 mg/kg i.p. completely protected animals from MES-induced seizures but also killed one animal and induced neurological deficits in 4/4 animals. Subsequent quantitative evaluation of riluzole in the mouse MES test rendered an $ED_{50}$ of 4.07 mg/kg (95 % CI 3.28–4.85; 6 doses, $n$=8 per dose) and a $TD_{50}$ of 17.27 mg/kg (95 % CI 15.58–19.14; 6 doses, $n$=8). Riluzole was further looked at after oral application in rats, where it was found to have an $ED_{50}$ of 2.64 mg/kg (95 % CI 1.81–3.75; 4 doses, $n$=8 per dose) and a $TD_{50}$ of 21.44 mg/kg (95 % CI 14.59–27.85). Riluzole was also much better tolerated in mice after oral application ($TD_{50}$ 55.26 mg/kg; 95 % CI 46.35–65.98). Based on this much better oral tolerability and the MES experiments (shown in Fig. 5) showing no significant difference in the toxicity of SKA-19 and riluzole when administered as solutions, we believe that there is no substantial difference in the relative toxicity of the 2 compounds and that the differences observed in the initial screen were probably caused by quicker absorption of riluzole out of the methylcellulose suspension used by the ASP. In keeping with this notion, riluzole typically reached its maximal effect more quickly (0.25 or 0.5 h) than SKA-19. Like SKA-19, riluzole showed no significant activity in the PTZ test.

## SKA-19 is Active in the 6-Hz Seizure Test, Hippocampal Kindled Rats, and the Frings AGS Susceptible Mouse Model

SKA-19 was also examined in an alternative electroshock test, the 6-Hz seizure test in mice. The 6-Hz test is a limbic seizure model induced by a low frequency, long-duration stimulus delivered by a corneal electrode [16]. It produces an initial stun followed by vibrissae chombing, forelimb clonus, and a Straub tail. In an initial screen SKA-19 exhibited full protection (4/4 animals) 2 h after i.p. administration of 10 mg/kg and partial protection at all other tested time points. Subsequent quantitative testing of multiple doses at the 2 h time point (Fig. 3a) gave an $ED_{50}$ of 12.19 mg/kg (95 % CI 8.2–17.45; $n$=8 per dose). A second set of 6-Hz experiments was performed with a higher current intensity of 44 mA at which the

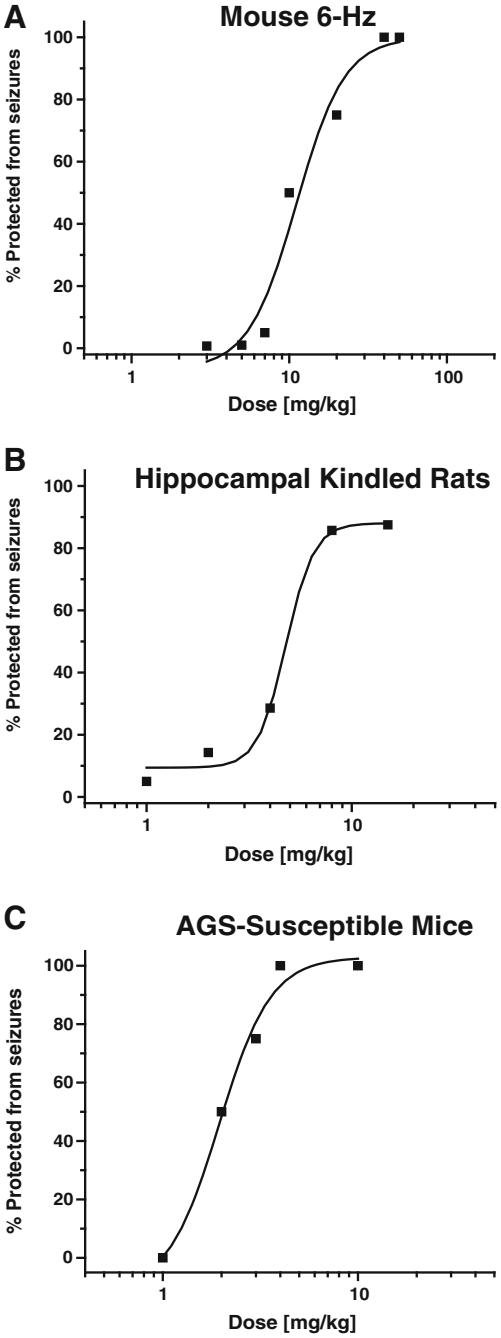


**Fig. 3** 2-Amino-6-trifluoromethylthio-benzothiazole (SKA-19) shows efficacy in multiple seizure models. (**a**) 6-Hz seizure test in mice: $ED_{50}$ 12.19 mg/kg [95 % confidence interval (CI) 8.2–17.45, $n$=8 per dose]. See Fig. 2 for mouse $TD_{50}$ 2 h after intraperitoneal (i.p.) application. (**b**) Hippocampal kindled rats: $ED_{50}$ 5.47 mg/kg (95 % CI 2.92–8.92, $n$=8 per dose). (**c**) Frings audiogenic seizure (AGS)-susceptible mouse model: $ED_{50}$ 2.15 mg/kg (95 % CI 1.52–2.65, $n$=8 per dose). In all cases, testing was performed 2 h after i.p. application of SKA-19

6-Hz test becomes more discriminatory and has been suggested as a model for therapy-resistant seizures [20]. At this higher current intensity SKA-19 was found to exhibit an $ED_{50}$ of 28.15 mg/kg (95 % CI 18.14–46.78; $n$=8 per dose). However, it should be noted when judging the 6-Hz test that SKA-19 was tested at 5, 10, 20, 40, and 60 mg/kg, and that the 40 and 60 mg/kg doses are above the $TD_{50}$ (29.73 mg/kg) for affecting mouse rotorod performance. Orally administered riluzole exhibited similar efficacy in the 6-Hz test, but reached its peak effect earlier than SKA-19 ($ED_{50}$ 10.1 mg/kg with a current intensity of 32 mA, and 11.54 mg/kg with a current intensity of 44 mA at the 0.5-h and 1-h time points, respectively).

SKA-19 was next evaluated in hippocampal kindled rats, a model that can predict efficacy of an AED for treating complex partial seizures and preventing seizure spread from a focus [1, 16]. In a preliminary experiment with 2 fully kindled rats SKA-19 at 30 mg/kg i.p. reduced the predrug seizure score from 4–5 to 0 and completely suppressed the afterdischarge duration. As shown in Fig. 3b, a quantitative test of increasing doses in kindled rats determined an $ED_{50}$ of 5.47 mg/kg (95 % CI 2.92–8.92; $n$=8 per dose) with no evidence of toxicity at the highest dose (15 mg/kg) in these "seizure experienced animals", despite the fact that this dose was similar to the previously determined $TD_{50}$ in normal, not kindled, rats (see Fig. 2b). In lamotrigine-resistant amygdala-kindled rats, SKA-19 only exhibited partial protection with 2/8 rats protected at 6 mg/kg and 3/7 fully kindled rats protected at 50 mg/kg.

SKA-19 was further evaluated in the Frings AGS-susceptible mouse model [18]. Frings AGS-susceptible mice exhibit sound-induced seizures, which manifest as wild running, loss of righting reflex, tonic flexion, and tonic extension in response to high-intensity sound stimulation such as a 20-s 110 decibels sound. While the model typically does not differentiate well between different anticonvulsants and is not useful for identifying compounds effective in difficult-to-treat partial seizures [21], its utility rests in its usefulness at predicting potential efficacy against hereditary epilepsy. As shown in Fig. 3c, SKA-19 protected Frings AGS-susceptible mice from sound induced seizures with an $ED_{50}$ of 2.15 mg/kg (95 % CI 1.52–2.65; $n$=8 per dose).

## SKA-19 Does Not Affect Seizure Threshold in the i.v. PTZ Test

As some anticonvulsants can paradoxically reduce seizure threshold and thus exhibit proconvulsant activity under certain circumstances, SKA-19 was evaluated in the i.v. PTZ test, which determines whether a compound reduces or increases the time to the first twitch or to clonus during a continuous i.v. infusion of PTZ. Vehicle or SKA-19 at 5 and 30 mg/kg, doses corresponding to the mouse MES $ED_{50}$ and the mouse $TD_{50}$ (Fig. 2), were administered i.p. to mice ($n$=10 per group). The lower dose did not change the time to the first twitch or clonus, while the higher dose increased both slightly [PTZ to first twitch: vehicle 28.0±0.96 mg/kg, SKA-19 31.6±1.0 mg/kg ($p$=0.008); PTZ dose to first clonus: vehicle 30.6±1.19 mg/kg, SKA-19 37.2±1.25 mg/kg (p=0.000)]. This slight elevation in threshold at 30 m/kg is in keeping with SKA-19 having antiseizure activity and demonstrates that SKA-19 is not proconvulsant.

## Pharmacokinetics of SKA-19

The anticonvulsant testing at the ASP had shown that SKA-19 must have a relatively good bioavailability as it was effective following both oral and i.p. application as a suspension in 0.5 % methylcellulose. Activity typically peaked between 1 and 2 h and lasted 4 h, sometimes even longer as in the case of the sedation and neurological impairment, which were observable for up to 24 h following administration of 200 mg/kg SKA-19 in the toxicity studies. This prolonged effect suggested a half-life somewhere between 1 and 3 h. In order to determine the pharmacokinetic properties of SKA-19 we established an ultra performance liquid chromatography/MS assay based on a high-performance liquid chromatography/MS assay we had previously published for the benzothiazole SKA-31 [13], and determined total SKA-19 plasma concentrations in rats following i.v., i.p,. and oral application as solution. Following i.v. administration at 10 mg/kg ($n$=3), SKA-19 plasma concentrations fell biexponentially, reflecting a 2-compartment model with very rapid distribution from blood into tissue followed by elimination with a half-life of 2.2 h (Fig. 4a). Following oral administration of a solution of 10 mg/kg, SKA-19 plasma concentrations stayed around 1 μM for 5 h and then fell to 0.4 μM at 8 h (Fig. 4b). Gavage of SKA-19 as a suspension in methylcellulose as used by the ASP resulted in a very similar plasma concentrations (Fig. 4b). The plasma peak was slightly delayed and the peak concentration slightly higher (1.6±0.6 μM); however, the overall exposure level was not significantly different. Oral availability was found to be roughly 30 % in both vehicles.

We further injected SKA-19 i.p. at doses of 10 and 30 mg/kg (Fig. 4c). In keeping with the high total plasma concentrations measured at 2 h (11.96±2.21 μM; $n$=3) and 4 h (13.09±2.67 μM), rats receiving 30 mg/kg showed prolonged sedation but recovered without weight loss at 24 h. Tissue concentration determinations performed 2 h after i.p. application of 10 mg/kg revealed that SKA-19 is very effective at penetrating into tissues such as brain, heart, spleen, and liver (Fig. 4c). A direct comparison with the same dose of riluzole (10 mg/kg i.p.), which resulted in very similar plasma concentrations at 2 h (4.6±1.3 μM for SKA-19 and 4.1±0.2 μM for riluzole), showed that SKA-19 reached roughly 3-fold higher brain than plasma concentrations, while riluzole

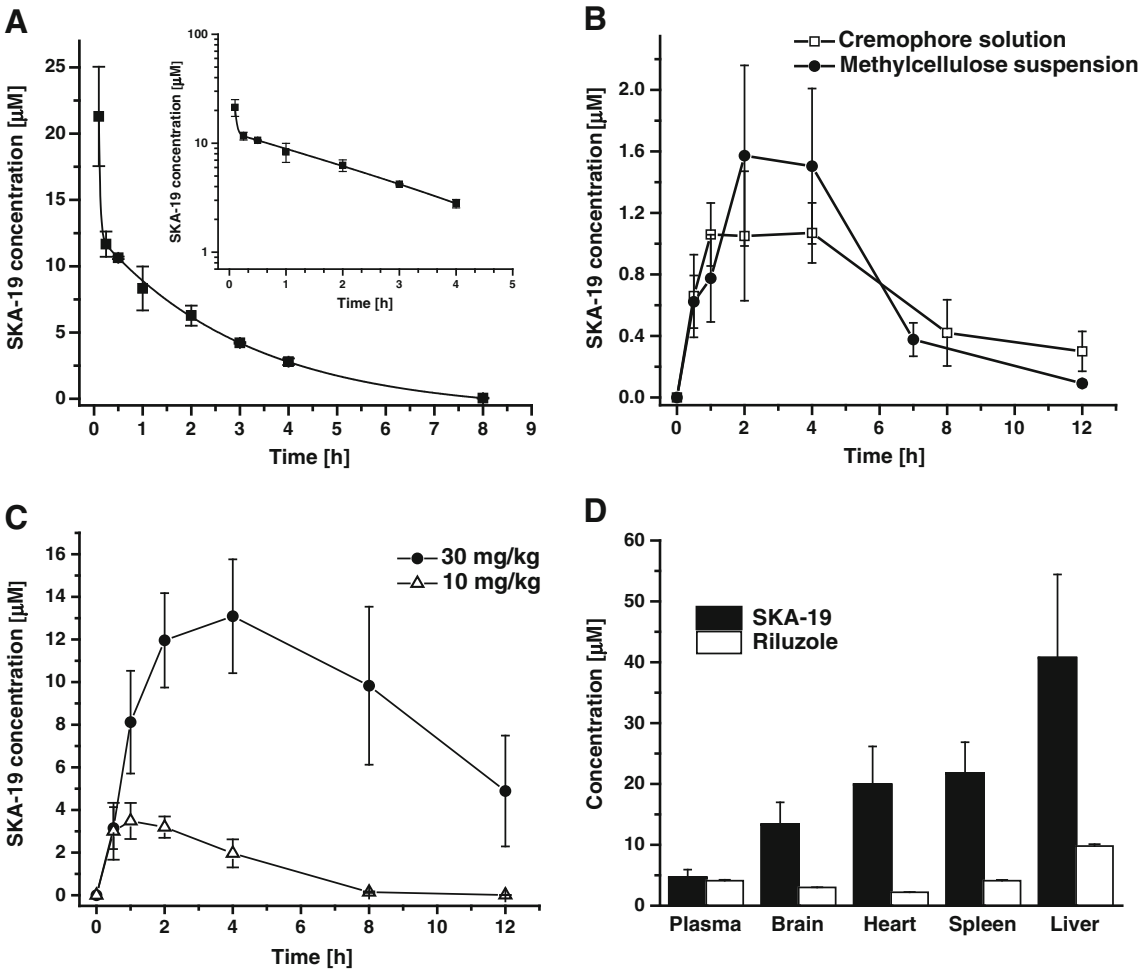


**Fig. 4** Pharmacokinetics of 2-amino-6-trifluoromethylthiobenzothiazole (SKA-19). (**a**) Total SKA-19 plasma concentrations (mean±SD) following intravenous administration of 10 mg/kg in CremophorEL (Sigma-Aldrich, St. Louis, MO, USA)/phosphate-buffered saline to male Sprague–Dawley rats ($n$=3). The inset shows the same data on a log scale. The data were best fitted as biexponential decay and with a quick distribution into tissue followed by elimination ($t_{1/2}$= 2.16±0.023 h). (**b**) SKA-19 plasma concentrations following oral gavage application at 10 mg/kg in solution ($n$=3) or as a methylcellulose suspension ($n$=3). (**c**) Plasma concentrations following intraperitoneal (i.p.) application at 10 and 30 mg/kg ($n$=3). (**d**) Tissue concentrations 2 h after i.p. administration of SKA-19 and riluzole at 10 mg/kg ($n$=3)

exhibited a brain plasma ratio of 1:1 in our hands (Fig. 4c). We further determined the plasma protein binding of SKA-19 and found 82 % bound with rat plasma.

## Direct Comparison of Riluzole and SKA-19 in MES Seizure Test

In order to directly compare SKA-19 and riluzole we next performed a set of MES experiments in mice. Both SKA-19 and riluzole were administered i.p. as solutions in a volume of 10 ml/kg to assure quick and efficient absorption. Protection from seizures induced by corneal electrodes was seen as early as 5 min after application of both compounds (Fig. 5). However, riluzole only provided a relatively short-lived protection and even 10 mg/kg was not protective for longer than 45 min (Fig. 5a). In contrast, SKA-19 provided full protection for 2.5 h at the 10 mg/kg dose and significant seizure protection at 5 and 6 mg/kg for at least 90 min (Fig. 5c). Quantitative testing at the 10 min time point rendered an $ED_{50}$ of 4.93 mg/kg (95 % CI 4.15–5.86; $n$=6–8 per dose) and a $TD_{50}$ of 16.08 (95 % CI 13.06–19.02) for SKA-19, and very similar $ED_{50}$ and $TD_{50}$ values for riluzole (Fig. 5b, d).

The PI ($TD_{50}/ED_{50}$) for SKA-19 in these experiments was lower (PI 3.2) than with the suspension preparation used by the ASP but the $ED_{50}$ was identical to the mouse $ED_{50}$ determined in the MES test by the ASP at 2 h, suggesting that the severity of the neurological impairment induced by SKA-19 depends, in part, on how quickly brain concentrations rise. The brain is a well perfused organ and following i.p. administration of SKA-19 in a high volume, brain concentrations are likely to rise much more quickly than after i.p. administration of a suspension. In keeping with this interpretation, SKA-19 displayed the lowest toxicity following oral application. In this case, the PI was found to be 33 (Fig. 2c), probably

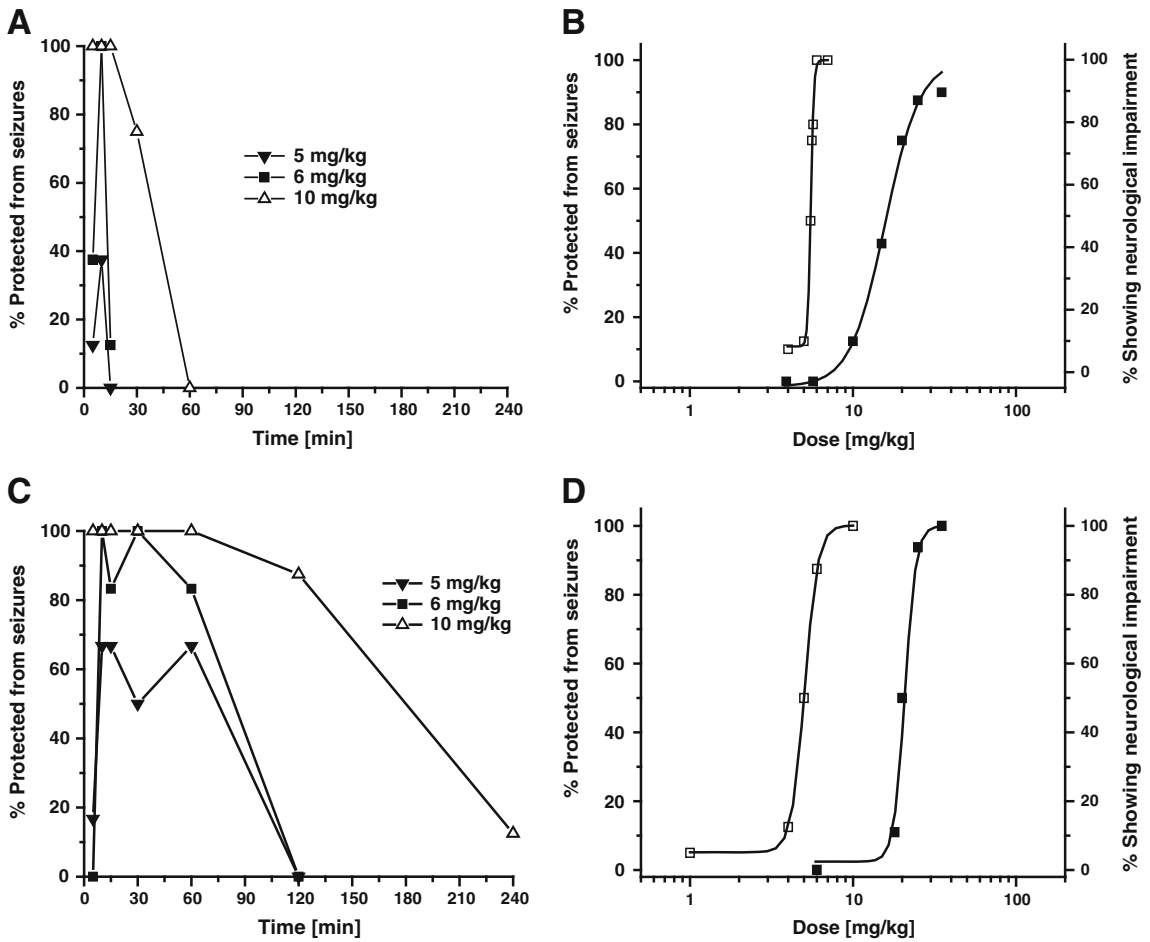


**Fig. 5** Comparison of seizure protection time course between riluzole and 2-amino-6-trifluoromethylthio-benzothiazole (SKA-19). (**a**) Time course of seizure protection in the mouse maximal electroshock (MES) test following intraperitoneal (i.p.) administration of riluzole as a solution ($n$=8 per time point). (**b**) Dose–response curves for seizure protection in MES test (□) and neurological impairment (■) following i.p. administration of increasing riluzole doses in mice ($n$=8 per dose, 10-min time point). $ED_{50}$ 5.37 mg/kg [95 % confidence interval (CI) 5.17–5.57], $TD_{50}$ 15.77 mg/kg (95 % CI 11.94–20.83); protective index (PI) 2.9. (**c**) Time course of seizure protection in the mouse MES test following i.p. administration of SKA-19 as a solution ($n$=6–8 per time point). (**d**) Dose–response curves for seizure protection in MES test (□) and neurological impairment (■) following i.p. administration of increasing SKA-19 doses in mice ($n$=6–8 per dose, 10-min time point). $ED_{50}$ 4.93 mg/kg (95 % CI 4.15–5.86), $TD_{50}$ 16.08 mg/kg (95 % CI 13.06–19.02); PI 3.2

because brain concentrations rose more slowly in parallel with the slower rise in plasma concentrations observed after oral dosing (Fig. 4b).

## SKA-19 Shows Efficacy in Pain Models

Intraplantar injection of a dilute formalin solution (0.5 %) into the hindpaw induces a biphasic pain response in mice. Immediately following the injection the mouse intensely lifts, licks, and flicks the paw for approximately 5–10 min. This first phase (phase I) is thought to result from a direct activation of primary afferent neurons and has recently been shown to be largely caused by direct stimulation of transient receptor potential cation channel, member A1 (TRPA1) [22]. After a brief latent period where there is little behavioral activity, a more prolonged second phase (phase II) of about 30–60 min of activity then ensues, which is characterized by sensitization of CNS neurons in the dorsal horn, continuing afferent input, and inflammation. SKA-19 administration at 5 mg/kg 2 h prior to formalin injection significantly decreased nociceptive behavior measured as the amount of time animals spent licking the affected hindpaw in a 2-min period recorded at 5-min intervals in phase I and the early phase II (Fig. 6a). Quantification by determining the area under curve showed a 54.5 % reduction of the total paw licking in phase I ($n$=8 per group; $p$<0.05) and a 31.3 % reduction of paw licking in phase II ($p$<0.05), which the individual time points showing significant reductions up to 20 min.

SKA-19 was further evaluated for its ability to raise allodynic threshold in a Von Frey test following partial sciatic nerve ligation in rats (Fig. 6b). The threshold for foot withdrawal in response to a series of calibrated Von Frey fibers was determined in rats 7 days after recovery from nerve ligation surgery ($n$=8). Subsequent SKA-19 administration at 5 mg/kg significantly increased the withdrawal threshold at the 2-h time point.

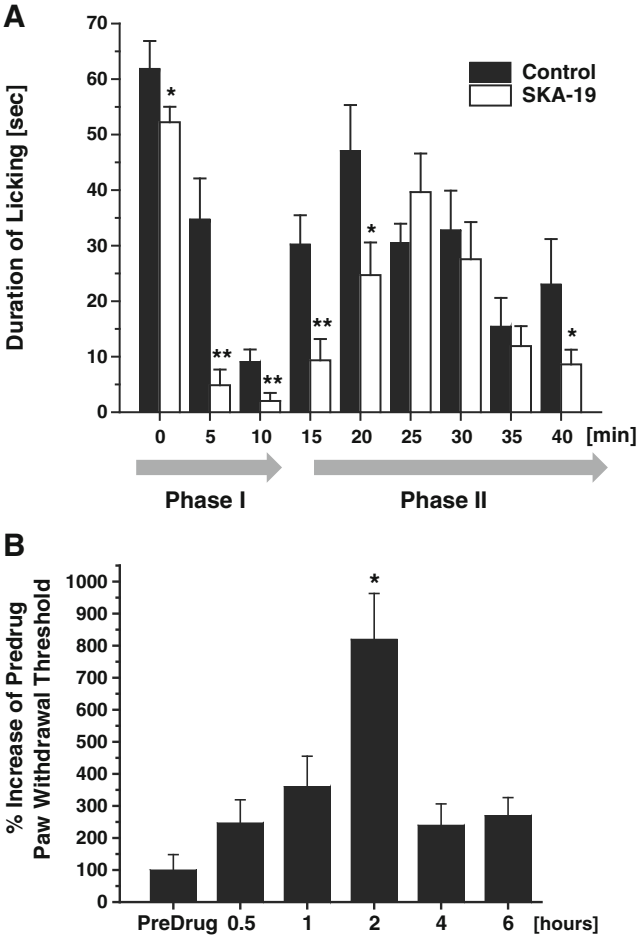


**Fig. 6** 2-Amino-6-trifluoromethylthio-benzothiazole (SKA-19) is effective in pain models. (**a**) SKA-19 (5 mg/kg administered 2 h prior to formalin injection) significantly decreased the time mice spent licking the affected hindpaw in a 2-min period recorded at 5-min intervals in the formalin pain test ($n$=8 per group). (**b**) Threshold for foot withdrawal in response to a series of calibrated Von Frey fibers in rats 7 days ($n$=8) after recovery from nerve ligation surgery following administration of SKA-19 (5 m/kg)

## SKA-19 Reduces 4-AP and PTX-Induced $Ca^{2+}$ Oscillations in Hippocampal Neurons

In order to identify the mechanism of action of SKA-19, we started by testing its effect on neuronal $Ca^{2+}$ oscillations. Cultured hippocampal neurons display spontaneous synchronous $Ca^{2+}$ oscillations the frequency and amplitude of which can be monitored in real-time using FLIPR Tetra [19]. While SKA-19 concentrations of ≤1 did not significantly inhibit spontaneous $Ca^{2+}$ oscillations, SKA-19 concentrations of 3 μM or more completely eliminated spontaneous $Ca^{2+}$ oscillations (Fig. 7a), suggesting that SKA-19 affects neuronal excitability. We next investigated the effect of SKA-19 on $Ca^{2+}$ oscillations induced by the proconvulsant agents 4-AP and picrotoxin (PTX). While the $K^+$ channel blocker 4-AP produced an immediate elevation of neuronal intracellular $Ca^{2+}$ later followed by a drastically increased $Ca^{2+}$ oscillation frequency with lower amplitude (Fig. 7b), the gamma-aminobutyric acid (GABA) receptor A ($GABA_A$) blocker PTX caused a sharper and more transient rise in intracellular $Ca^{2+}$, which was followed by a decrease in the frequency but a rise in the amplitude of $Ca^{2+}$ oscillations (Fig. 7c). SKA-19 potently suppressed both the initial rise and the oscillations induced by both agents, suggesting that it significantly affects neuronal activities driving the $Ca^{2+}$ oscillations induced by 4-AP and PTX in these neuronal networks.

## SKA-19 Reduces AP Firing in CA1 Pyramidal Neurons by Inhibiting $Na_V$ Channels and Activating KCa2 Channels

As SKA-19 is a potent anticonvulsant in multiple seizure models and suppresses neuronal $Ca^{2+}$ oscillations, we next tested its effect on firing of CA1 pyramidal neurons in mouse hippocampal slices. Under normal conditions CA1 neurons started firing action potentials (APs) following injection of 30-pA current and subsequently fired APs with increasing frequency at higher current injections. Following a 1-s 150-pA current injection to elicit a series of APs, application of 1 μM SKA-19 slowed down AP firing, while 25 μM completely suppressed it (Fig. 8a). The intermediate concentration of 10 μM of SKA-19 reduced the number of spikes at all injected current levels by roughly 50 % (Fig. 8b). A close inspection of individual APs revealed that exposure to 10 μM SKA-19 was associated with an increase in after-hyperpolarization amplitude, suggesting that the effect of SKA-19 is at least partly due to the activation of KCa2 (=SK) channels. To provide support for this conclusion we compared the effect of SKA-19 with the effect of the more specific KCa2 channel activator NS309 (data not shown). At 10 μM, a concentration at which it had previously been shown to exert saturating effects on the medium afterhyperpolarization (mAHP) in CA1 pyramidal neurons in rat hippocampal slices [23], NS309 reduced AP firing frequency following 1-s current injections (150 pA) from a holding potential of –65 mV; however, unlike SKA-19 under the same conditions, it did not terminate firing during the ongoing current train, suggesting that SKA-19 has additional effects on other channels than KCa2 channels. To confirm that SKA-19 reduces neuronal firing at least partly by enhancing KCa2 channel activity, we directly measured the mAHP current in the presence or absence of SKA-19 in voltage–clamp experiments. SKA-19 induced a modest but significant increase in the mAHP amplitude compared with control (Fig. 8c). We next tested SKA-19 on KCa2 channels stably expressed in HEK-293 cells. In whole-cell patch–clamp recordings SKA-19 potentiated KCa2.2 (SK2) and KCa2.3 (SK3) currents elicited by 250 nM of free intracellular $Ca^{2+}$ with $EC_{50}$ values of 14 and 15 μM (Fig. 8d, e; Table 1). Similar to other positive KCa channel gating modulators like SKA-31 and NS309 [13], SKA-19 maximally increased KCa2 currents 30-fold at this intracellular $Ca^{2+}$ concentration. Interestingly,

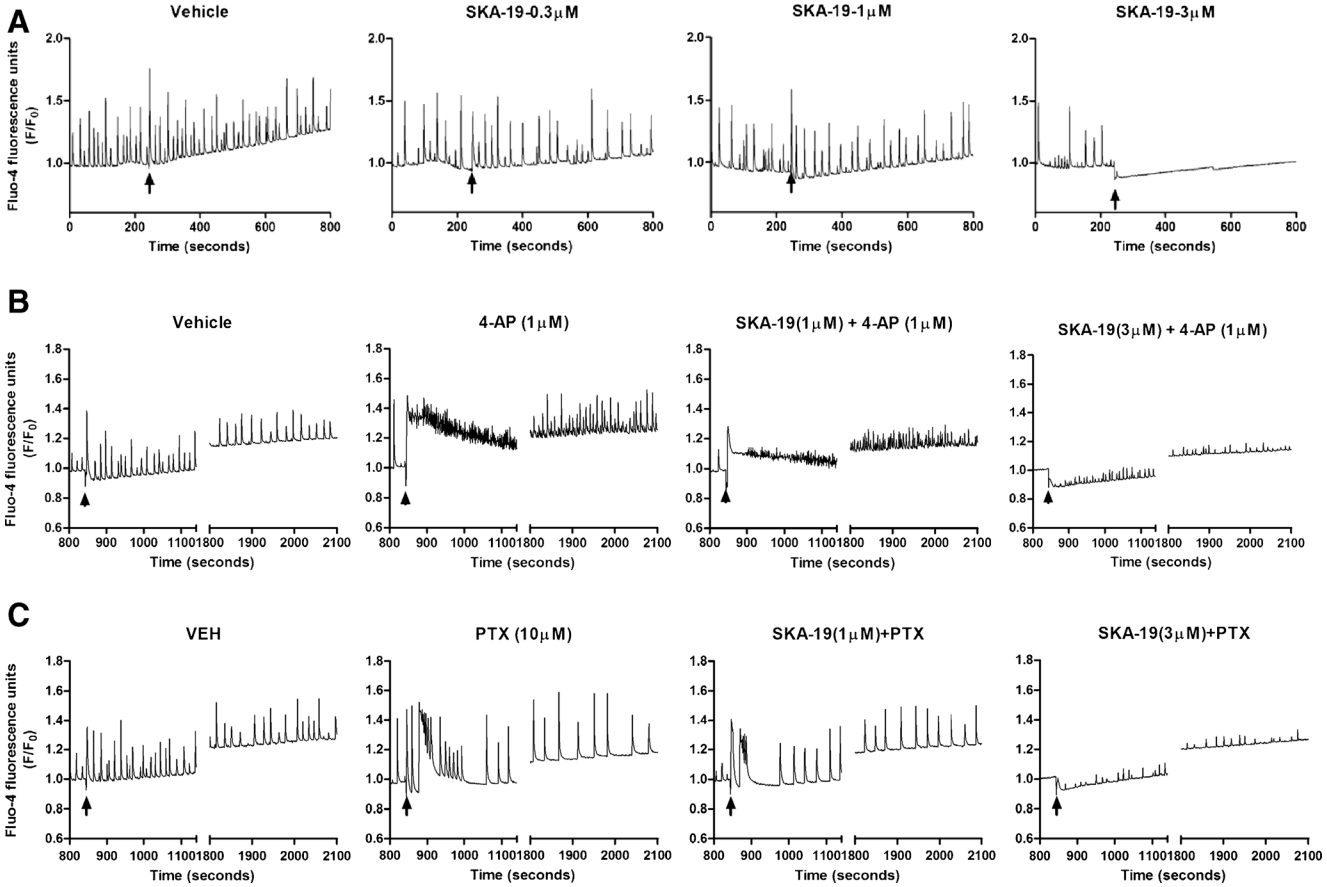


**Fig. 7** Increasing concentrations of 2-amino-6-trifluoromethylthiobenzothiazole (SKA-19) inhibit (**a**) spontaneous, and (**b**) 4-aminopyridine (4-AP)- and (**c**) picrotoxin-induced $Ca^{2+}$ oscillations in cultured 14 days *in vitro* (DIV) hippocampal neurons. (**a**) SKA-19 concentrations of 1 μM or less have no effect on spontaneous $Ca^{2+}$ oscillations. The arrow indicates addition of SKA-19. (**b**) 4-AP (1 μM, arrow indicates addition) produces an immediate but transient elevation in neuronal intracellular $Ca^{2+}$ followed by increased $Ca^{2+}$ oscillation frequency with lower amplitude. The initial rise and the oscillations are inhibited by SKA-19. SKA-19 was added 10 min before 4-AP. (**c**) Picrotoxin (PTX; 10 μM, arrow indicates addition) induces higher amplitude $Ca^{2+}$ oscillations, which are inhibited by SKA-19 (added 10 min before PTX). VEH=vehicle

SKA-19 displayed selectivity for KCa2.2 and KCa2.3 over KCa2.1, and only showed very weak effects on KCa2.1 currents at concentrations of 100 and 200 μM (Fig. 8e).

Based on its structural similarity to riluzole, its sedating properties at higher concentrations and its pronounced effects on neuronal firing (Fig. 8a, b), we further suspected that SKA-19 would also block $Na_V$ channels and therefore investigated its blocking properties on several sodium channel isoforms. SKA-19 inhibited $Na_V1.1$ and $Na_V1.2$, 2 of the major neuronal sodium channels, with $IC_{50}$ values of approximately 7.90 ±0.01 μM (Fig. 8f; Table 1) when cells were held at –90 mV and pulsed with a frequency of 0.1 Hz. Changing the holding potential or the pulse frequency to 20 Hz revealed that inhibition by SKA-19 was highly state- and use-dependent as both manipulations significantly affected the $IC_{50}$ for $Na_V1.2$ by lowering it to 860 or 520 nM, respectively (Fig. 8f). As expected, SKA-19 did not exhibit any selectivity among sodium channel isoforms and also blocked $Na_V1.4$, $Na_V1.5$, and $Na_V1.7$ in the low micromolar range (Table 1). Taken together, SKA-19 therefore seems to be a "dirty" ion channel modulator that exerts its anticonvulsant and analgesic effects through a combination of KCa2 channel-activating and $Na_v$ channel-blocking activity.

## Discussion

Epilepsy and neuropathic pain are characterized by abnormal excessive or ectopic neuronal excitability. Drugs currently used in the clinic to treat epilepsy include inhibitors of voltage-gated $Na^+$ and $Ca^{2+}$ channels, activators of voltage-gated $K^+$ channels, and modulators of GABAergic inhibitory and glutamatergic excitatory neurotransmission [24], while the anticonvulsants gabapentin, pregabalin, carbamazepine, and lamotrigine are also used for the treatment of neuropathic pain [25]. We here describe the discovery of SKA-19, a thioanalog of riluzole, which is orally available, brain penetrant, and displays activity in several rodent seizure models. SKA-19 has a dual mechanism of action and is both a use- and

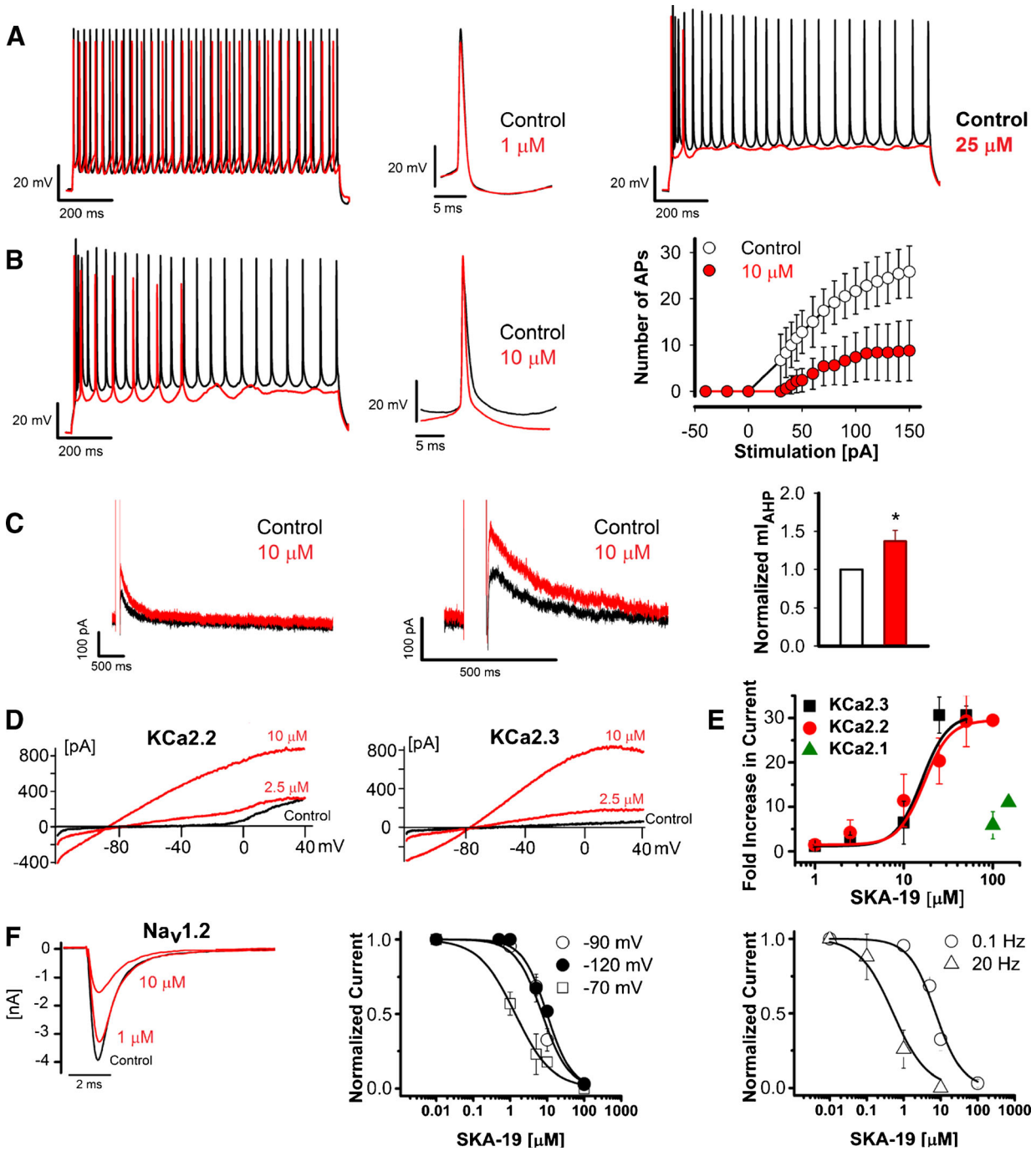


**Fig. 8** 2-Amino-6-trifluoromethylthio-benzothiazole (SKA-19) reduces action potential (AP) firing of hippocampal pyramidal neurons by activating KCa2 channels and inhibiting voltage-gated $Na^+$ channels ($Na_V$) channels. (**a**) Overlay of representative AP traces recorded before (black) and after (red) perfusion of 1 μM SKA-19 (left) or 25 μM SKA-19 (right). Cells were held at –65 mV and a train of APs evoked by a 1-s 150-pA current injection. (**b**) Overlay of AP traces recorded in the absence and presence of 10 μM SKA-19 (left), and plot of the number of APs elicited in the presence (red) and absence of SKA-19 in response to stimulating current injections of increasing amplitude (right). Data points represent means and SDs for 3 independent neurons. (**c**) SKA-19 enhances the medium afterhyperpolarization (AHP). SKA-19 at a concentration of 10 μM increases the amplitude of the current underlying the medium AHP. Shown on a compressed (left) and expanded time scale (middle). Bar graph of normalized $mI_{AHP}$ current amplitude (right). Shown are means and SDs for 3 neurons. (**d**) SKA-19 activates rKCa2.2 and hKCa2.3 stably expressed in human embryonic kidney-293 cells. (**e**) Concentration–response curve for the activation of KCa2.1, KCa2.2, and KCa2.3 recorded in the presence of 250 nM of free intracellular $Ca^{2+}$. See Table 1 for $EC_{50}$ values. (**f**) SKA-19 is a state- and use-dependent inhibitor of Nav1.2 currents in N1E-115 neuroblastoma cells. Sample $Na_V1.2$ current traces blocked by 1 μM and 10 μM SKA-19 (left). State-dependence (middle): $IC_{50}$ at –70 mV holding potential is 0.86± 0.70 μM; $IC_{50}$ at –90 mV holding potential is 7.90±0.01 μM; $IC_{50}$ at –120 mV holding potential is 9.50±1.72 μM. Use-dependence (right): $IC_{50}$ at 0.1 Hz is 7.90±0.01 μM; $IC_{50}$ at 20 Hz is 0.52±0.23 μM. Data points represent means plus SDs extracted from recordings from at least 3 independent cells

**Table 1** Selectivity of 2-amino-6-trifluoromethylthio-benzothiazole

| Channels | $EC_{50}$ or $IC_{50}$ (μM) | *n* |
|---|---|---|
| KCa2.1 | > 100 | 5 |
| KCa2.2 | 14±5 | 12 |
| KCa2.3 | 15±5 | 14 |
| $Na_V1.1$ | 6.9±4.9 | 5 |
| $Na_V1.2$ | 7.9±0.02 | 3 |
| $Na_V1.4$ | 2.2±1.1 | 6 |
| $Na_V1.5$ | 4.5±2.7 | 7 |
| $Na_V1.7$ | 5.8±2.6 | 3 |
| $K_V2.1$ | 22.3±5.6 | 3 |

*n* number of cells used per experiment

state-dependent $Na_V$ channel blocker and an activator of small-conductance $Ca^{2+}$-activated KCa2 $K^+$ channels. Through this dual mechanism SKA-19 reduces neuronal excitability in 2 ways: it decreases firing frequency and increases medium after-hyperpolarization. Both targets, $Na_V$ and KCa2 channels, are expressed at high levels in the brain, including in regions relevant to seizure disorders, such as cortex, hippocampus, and thalamus. $Na_V1.1$ and $Na_V1.2$ may play an important role in the control of neuronal excitability and epileptiform activity [26]. More than 100 different mutations in the genes encoding $Na_V1.1$ and $Na_V1.2$, *SCNA1* and *SCNA2*, have been identified in patients with genetic epilepsy with febrile seizures. Missense mutations in *SCN2A* have further been found in patients with benign familial neonatal convulsions [27], while *SCNA1* mutations also seem to cause 2 other severe epilepsy syndromes of early life: Dravet syndrome and intractable childhood epilepsy with generalized tonic–clonic seizure [26]. Another strong argument for the importance of $Na_V$ channels in seizures is, of course, the fact that many clinically used anticonvulsants such as lamotrigine, phenytoin, and carbamazepine target $Na_V$ channels [24].

Voltage-independent small-conductance $Ca^{2+}$-activated $K^+$ currents were first described in 1982 [28], and later found to be mediated by 3 closely related channels [29]: KCa2.1 (SK1 or KCNN1), KCa2.2 (SK2 or KCNN2), and KCa2.3 (SK3 or KCNN3). While KCa2.1 and KCa2.2 are particularly enriched in the cortex and the hippocampus, KCa2.3 is most prominet in subcortical areas like the striatum, thalamus, and monaminergic nuclei. KCa2 channels underlie the apamin-sensitive mAHP [30–32], and thus play an important role in controlling neuronal excitability and firing frequency. Pharmacological modulation of KCa channels therefore offers the opportunity to affect significantly neuronal activity. While KCa2 channel blockers like the bee venom toxin apamin increase firing rates, induce high frequency bursts in neurons that normally exhibit regular tonic action potential firing [33], and can elicit seizures in rodents [34], KCa2 channel activators reduce neuronal firing rates and suppress epileptiform activity in cultured hippocampal neurons [23, 35, 36]. KCa2 channel activators have therefore been proposed for the treatment of CNS disorders that are characterized by hyperexcitability, such as epilepsy and ataxia [15]. While the data supporting the use of KCa2 activators in ataxia are relatively strong [37–41], this approach has yet to be validated as a viable epilepsy treatment strategy. However, several lines of evidence lend credence to the idea that KCa2 channels may play a role in regulating seizure discharges and could therefore be a target for epilepsy drug treatment. Genetically epilepsy prone rats exhibit reduced afterhyperpolarization (AHP) currents resulting in a marked reduction in spike frequency adaptation in CA3 hippocampal neurons [42], and have more recently been found to express lower levels of KCa2.1 and KCa2.3 but higher levels of KCa2.2 in inferior colliculus neurons [43], suggesting that KCa2 channel dysregulation may contribute to the seizure susceptibility of these animals. It has further been shown that rats rendered chronically epileptic as a result of pilocarpine-induced status epilepticus exhibit significantly reduced KCa2-mediated AHP currents in CA1 hippocampal neurons [44]. Additionally, there is limited pharmacological evidence supporting the view that KCa2 is a relevant AED target. Several KCa2 activators suppress 4-AP induced epileptiform activities in rat hippocampal neurons [36], while 1-ethyl-2-benzimidazolinone (EBIO) and SKA-31 have been found to be effective in the MES test in mice [13, 45].

The anticonvulsant profile of SKA-19 is similar to the profile of "classical" sodium channel blocking anticonvulsants. SKA-19 is very effective in the MES test in mice and rats, AGS-susceptible mice, and hippocampal kindled rats [1, 16]. However, presumably owing to the additional KCa2 channel activating effect, SKA-19 has a broader profile than $Na_V$-channel blocking anticonvulsants. SKA-19 also shows efficacy in the 6-Hz psychomotor seizure test at both 32 and 44 mA, suggesting that it might have some utility for therapy-resistant seizures [20]. In lamotrigine-resistant amygdala kindled rats, SKA-19 exhibited partial protection but could not be tested at higher doses without inducing sedation. Interestingly, SKA-19 is ineffective against clonic seizures induced by the $GABA_A$ receptor antagonist PTZ, and, in this respect, is different from the clinically used $K^+$ channel activator retigabine (ezogabine), which activates Kv7.2–Kv7.5 (KCNQ2–KCNQ5) channels and which shows efficacy against $GABA_A$ receptor antagonist-induced seizures [24]. Out of the currently clinically used anticonvulsants, SKA-19 most closely matches the profiles of zonisamide and lacosamide, which both have a very similar anticonvulsant profile (i.e., activity in MES, 6-Hz, AGS, and kindled models but not against seizures induced by $GABA_A$ antagonists) and which both inhibit $Na_V$ channels, but are distinct from other $Na_V$ blockers by exerting additional effects [24].

In the commonly used formalin pain model, SKA-19 shows a profile that resembles other $Na_V$ channel blockers

but is, again, a little broader. Phase I in the formalin model is thought to result from an activation of primary afferent neurons through direct stimulation of the transient receptor potential family channel TRPA1 by formalin and is effectively suppressed by local anesthetics such as lidocaine, selective $Na_V1.7$ blockers, and TRPA1 antagonists [22, 46]. The subsequent phase II, which is characterized by sensitization of CNS neurons in the dorsal horn, continuing afferent input and inflammation, responds to opioid analgesics, *N*-methyl-D-aspartate antagonists, gabapentin, and nonsteroidal anti-inflammatory drugs. SKA-19 is similar to TRPA1 antagonists like HC-030031 in that it effectively suppresses pain responses in phase I and phase IIA but then loses efficacy in phase IIB [22]. Whether this loss of efficacy is simply due to falling plasma levels as SKA-19 was administered 2 h prior to the intraplantar formalin injection, increasing unspecific effects of formalin or a lack of effect of SKA-19 on later stages of the pain process will require further investigation. However, taken together, the results obtained from the formalin and sciatic ligation models demonstrate that SKA-19 exerts not only anticonvulsant, but also analgesic effects.

Based on our findings with SKA-19 we propose that compounds combining KCa2 channel-activating and $Na_v$ channel-blocking activity exert broad-spectrum anticonvulsant and analgesic effects. We would further like to point out that although SKA-19 exhibits a superior pharmacokinetic profile, especially better brain penetration, than its parent drug riluzole, riluzole essentially has the same pharmacological profile. Like SKA-19, riluzole is both a highly state- and use-dependent $Na_V$ blocker and a KCa2 channel activator, and we would like to suggest that riluzole, which is typically viewed as an amyotrophic lateral sclerosis drug, but has recently been reported to improve the symptoms of cerebellar ataxia [47], should be reinvestigated as a possible anticonvulsant and analgesic.

**Acknowledgments** This work was supported by the CounterACT Program, National Institutes of Health Office of the Director (NIH OD), and the National Institute of Neurological Disorders and Stroke (NINDS), grant numbers U54NS079202 and R21NS072585. N.C. was supported by a National Heart, Lung & Blood Institute T32 Training Program in Basic and Translational Cardiovascular Science (T32HL086350). B.M.B. was supported by a National Institute of General Medical Sciences-funded Pharmacology Training Program (T32GM099608). We are further highly indebted to the NIH Anticonvulsant Screening program. This work would not have been possible without their help.

**Required Author Forms** Disclosure forms provided by the authors are available with the online version of this article.

## References

1. Bialer M, White HS. Key factors in the discovery and development of new antiepileptic drugs. *Nat Rev Drug Discov* 2010;9:68-82.
2. Bialer M, Johannessen SI, Levy RH, Perucca E, Tomson T, White HS. Progress report on new antiepileptic drugs: a summary of the Eleventh Eilat Conference (EILAT XI). *Epilepsy Res* 2013;103:2-30.
3. Wickenden AD, Krajewski JL, London B, et al. *N*-(6-Chloro-pyridin-3-yl)-3,4-difluoro-benzamide (ICA-27243): A novel, selective KCNQ2/Q3 potassium channel activator. *Mol Pharmacol* 2008;73:977-986.
4. Roeloffs R, Wickenden AD, Crean C, et al. In vivo profile of ICA-27243 [*N*-(6-chloro-pyridin-3-yl)-3,4-difluoro-benzamide], a potent and selective KCNQ2/Q3 (Kv7.2/Kv7.3) activator in rodent anticonvulsant models. *J Pharmacol Exp Ther* 2008;326:818-828.
5. Dalby-Brown W, Jessen C, Hougaard C, et al. Characterization of a novel high-potency positive modulator of K(v)7 channels. *Eur J Pharmacol* 2013;709:52-63.
6. Biervert C, Schroeder BC, Kubisch C, et al. A potassium channel mutation in neonatal human epilepsy. *Science* 1998;279:403-406.
7. Mizoule J, Meldrum B, Mazadier M, et al. 2-Amino-6-trifluoromethoxy benzothiazole, a possible antagonist of excitatory amino acid neurotransmission. I. Anticonvulsant properties. *Neuropharmacology* 1985;24:767-773.
8. Rogawski MA. Epilepsy. In: *Neurotherapeutics: Emerging Strategies* Edited by Pullan L, Patel J. Totowa, NJ: Humana Press; 1996;193-273.
9. Gordon P, Corcia P, Meininger V. New therapy options for amyotrophic lateral sclerosis. *Expert Opin Pharmacother* 2013;14:1907-1917
10. Song JH, Huang CS, Nagata K, Yeh JZ, Narahashi T. Differential action of riluzole on tetrodotoxin-sensitive and tetrodotoxin-resistant sodium channels. *J Pharmacol Exp Ther* 1997;282:707-714.
11. Grunnet M, Jespersen T, Angelo K, et al. Pharmacological modulation of SK3 channels. *Neuropharmacology* 2001;40:879-887.
12. Duprat F, Lesage F, Patel AJ, Fink M, Romey G, Lazdunski M. The neuroprotective agent riluzole activates the two P domain K(+) channels TREK-1 and TRAAK. *Mol Pharmacol* 2000;57:906-912.
13. Sankaranarayanan A, Raman G, Busch C, et al. Naphtho[1,2-*d*-]thiazol-2-ylamine (SKA-31), a new activator of KCa2 and KCa3.1 potassium channels, potentiates the endothelium-derived hyperpolarizing factor response and lowers blood pressure. *Mol Pharmacol* 2009;75:281-295.
14. Adelman JP, Maylie J, Sah P. Small-conductance $Ca^{2+}$-activated $K^+$ channels: form and function. *Ann Rev Physiol* 2012:74:245-269.
15. Wulff H, Kolski-Andreaco A, Sankaranarayanan A, Sabatier JM, Shakkottai V. Modulators of small- and intermediate-conductance calcium-activated potassium channels and their therapeutic indications. *Curr Med Chem* 2007;14:1437-1457.
16. White HS, Woodhead JH, Wilcox KS, Stables J, Kuferberg H, Wolf HH. Discovery and preclinical development of antiepileptic drugs. In:. Levy RH, Mattson RH, Meldrum B, Perucca E (eds) Antiepileptic drugs, 5th edn. Lippincott Williams & Wilkins, Philadelphia, PA, 2002, pp. 36-48.
17. Kokate TG, Svensson BE, Rogawski MA. Anticonvulsant activity of neurosteroids: correlation with gamma-aminobutyric acid-evoked chloride current potentiation. *J Pharmacol Exp Ther* 1994;270:1223-1229.
18. Frings H, Frings M. Development of strains of albino mice with predictable susceptibilities to audiogenic seizures. *Science* 1953;117:283-284.
19. Cao Z, Hammock BD, McCoy M, Rogawski MA, Lein PJ, Pessah IN. Tetramethylenedisulfotetramine alters $Ca^{2+}$ dynamics in cultured hippocampal neurons: mitigation by NMDA receptor blockade and GABA(A) receptor-positive modulation. *Toxicol Sci* 2012;130:362-372.
20. Barton ME, Klein BD, Wolf HH, White HS. Pharmacological characterization of the 6 Hz psychomotor seizure model of partial epilepsy. *Epilepsy Res* 2001;47:217-227.
21. Bialer M, Twyman RE, White HS. Correlation analysis between anticonvulsant ED50 values of antiepileptic drugs in mice and rats

and their therapeutic doses and plasma levels. *Epilepsy Behav* 2004;5:866-872.
22. McNamara CR, Mandel-Brehm J, Bautista DM, et al. TRPA1 mediates formalin-induced pain. *Proc Natl Acad Sci USA* 2007;104;13525-13530.
23. Pedarzani P, McCutcheon JE, Rogge G, et al. Specific enhancement of SK channel activity selectively potentiates the afterhyperpolarizing current I(AHP) and modulates the firing properties of hippocampal pyramidal neurons. *J Biol Chem* 2005;280:41404-41411.
24. Porter RJ, Dhir A, Macdonald RL, Rogawski MA. Mechanisms of action of antiseizure drugs. *Handb Clin Neurol* 2012;108:663-681.
25. Rogawski MA, Loscher W. The neurobiology of antiepileptic drugs for the treatment of nonepileptic conditions. *Nat Med* 2004;10:685-692.
26. Meldrum BS, Rogawski MA. Molecular targets for antiepileptic drug development. *Neurotherapeutics* 2007;4:18-61.
27. Meisler MH, Kearney JA. Sodium channel mutations in epilepsy and other neurological disorders. *J Clin Invest* 2005;115:2010-2017.
28. Hugues M, Schmid H, Romey G, Duval D, Frelin C, Lazdunski M. The $Ca^{2+}$-dependent slow $K^+$ conductance in cultured rat muscle cells: characterization with apamin. *EMBO J* 1982;1:1039-1042.
29. Kohler M, Hirschberg B, Bond CT, et al. Small-conductance, calcium-activated potassium channels from mammalian brain. *Science* 1996;273:1709-1714.
30. Stocker M, Krause M, Pedarzani P. An apamin-sensitive $Ca^{2+}$-activated $K^+$ current in hippocampal pyramidal neurons. *Proc Natl Acad Sci USA* 1999;96:4662-4667.
31. Villalobos C, Shakkottai VG, Chandy KG, Michelhaugh SK, Andrade R. SKCa channels mediate the medium but not the slow calcium-activated afterhyperpolarization in cortical neurons. *J Neurosci* 2004;24:3537-3542.
32. Bond CT, Herson PS, Strassmaier T, et al. Small conductance $Ca^{2+}$-activated $K^+$ channel knock-out mice reveal the identity of calcium-dependent afterhyperpolarization currents. *J Neurosci* 2004;24:5301-5306.
33. Edgerton JR, Reinhart PH. Distinct contributions of small and large conductance $Ca^{2+}$-activated K+channels to rat Purkinje neuron function. *J Physiol* 2003;548:53-69.
34. McCown TJ, Breese GR. Effects of apamin and nicotinic acetylcholine receptor antagonists on inferior collicular seizures. *Eur J Pharmacol* 1990;187:49-58.
35. Pedarzani P, Mosbacher J, Rivard A, et al. Control of electrical activity in central neurons by modulating the gating of small conductance $Ca^{2+}$-activated $K^+$ channels. *J Biol Chem* 2001;276:9762-9769.
36. Kobayashi K, Nishizawa Y, Sawada K, Ogura H, Miyabe M. $K^+$-channel openers suppress epileptiform activities induced by 4-aminopyridine in cultured rat hippocampal neurons. *J Pharmacol Sci* 2008;108:517-528.
37. Walter JT, Alvina K, Womack MD, Chevez C, Khodakhah K. Decreases in the precision of Purkinje cell pacemaking cause cerebellar dysfunction and ataxia. *Nat Neurosci* 2006;9:389-397.
38. Alvina K, Khodakhah K. KCa channels as therapeutic targets in episodic ataxia type-2. *J Neurosci* 2010;30:7249-7257.
39. Shakkottai VG, Chou CH, Oddo S, et al. Enhanced neuronal excitability in the absence of neurodegeneration induces cerebellar ataxia. *J Clin Invest* 2004;113:582-590.
40. Shakkottai VG, do Carmo Costa M, Dell'Orco JM, et al. Early changes in cerebellar physiology accompany motor dysfunction in the polyglutamine disease spinocerebellar ataxia type 3. *J Neurosci* 2011;31:13002-13014.
41. Kasumu AW, Hougaard C, Rode F, et al. Selective positive modulator of calcium-activated potassium channels exerts beneficial effects in a mouse model of spinocerebellar ataxia type 2. *Chem Biol* 2012;19:1340-1353.
42. Verma-Ahuja S, Evans MS, Pencek TL. Evidence for decreased calcium dependent potassium conductance in hippocampal CA3 neurons of genetically epilepsy-prone rats. *Epilepsy Res* 1995;22:137-144.
43. N'Gouemo P, Yasuda RP, Faingold CL. Protein expression of small conductance calcium-activated potassium channels is altered in inferior colliculus neurons of the genetically epilepsy-prone rat. *Brain Res* 2009;1270:107-111.
44. Schulz R, Kirschstein T, Brehme H, Porath K, Mikkat U, Köhling R. Network excitability in a model of chronic temporal lobe epilepsy critically depends on SK channel-mediated AHP currents. *Neurobiol Dis* 2012;45:337-347.
45. Anderson NJ, Slough S, Watson WP. In vivo characterisation of the small-conductance KCa (SK) channel activator 1-ethyl-2-benzimidazolinone (1-EBIO) as a potential anticonvulsant. *Eur J Pharmacol* 2006;546:48-53.
46. Yang S, Xiao Y, Kang D, et al. Discovery of a selective NaV1.7 inhibitor from centipede venom with analgesic efficacy exceeding morphine in rodent pain models. *Proc Natl Acad Sci USA* 2013;110:17534-17539.
47. Ristori G, Romano S, Visconti A, et al. Riluzole in cerebellar ataxia: a randomized, double-blind, placebo-controlled pilot trial. *Neurology* 2010;74:839-845.